Density Functional Theory Study for the Cycloaddition of 1,3-Butadienes with Dimethyl Acetylenedicarboxylate. Polar Stepwise vs Concerted Mechanisms

Luis R. Domingo,*,† Manuel Arnó,‡ Renato Contreras,*,§ and Patricia Pérez[||]

Instituto de Ciencia Molecular and Departamento de Química Orgánica, Universidad de Valencia, Dr. Moliner 50, 46100 Burjassot, Valencia, Spain, Departamento de Química, Facultad de Ciencias, Universidad de Chile, Casilla 653-Santiago, Chile, and Departamento de Química Física, Facultad de Química, Pontificia Universidad Católica de Chile, Casilla 306, Correo 22, Santiago, Chile

Received: July 10, 2001; In Final Form: September 7, 2001

The molecular mechanisms for the cycloaddition reactions of four low activated 1,3-butadiene systems (1,3-butadiene, (*E*)-1,3-pentadiene, (*Z*)-1,3-pentadiene, and 4-methyl-1,3-pentadiene) with dimethyl acetylenedicarboxylate (DMAD) have been studied using density functional theory methods. For these cycloadditions, two competitive mechanisms have been characterized: the first one corresponds to a concerted C−C bond-formation where the asynchronicity depends on the methyl substitution. The second one corresponds to a stepwise process with a larger polar character where first a C−C bond is formed along the nucleophilic attack of 1,3-butadiene system to a conjugate position of the electron-poor substituted acetylene. Although the nonactivated 1,3-butadiene prefers the concerted process, substitution of hydrogen atoms by electron-releasing methyl groups favors the stepwise mechanism along with an increase of the charge-transfer process. A conformational analysis for DMAD reveals that both planar and perpendicular arrangements of the two-carboxylate groups have a decisive role on the dienophile/electrophile nature of this acetylene derivative. Thus, although the planar arrangement is preferred along the concerted process, the perpendicular favors the polar one along an increase of the electrophilicity of DMAD. The global and local electrophilicity power of these 1,3-butadienes and DMAD have been evaluated in order to rationalize these results. The study is completed with an analysis of the electrophilic/nucleophilic site activation, by probing the variations in local properties of DMAD perturbed by a model nucleophile with reference to a model transition structure. Inclusion of solvent effects, by means of a polarizable continuum model, does not modify these gas-phase results.

Introduction

The Diels−Alder (DA) reaction is among the most powerful C−C bond forming process and one of the widely studied transformations in organic chemistry. It corresponds to one of the general class of cycloaddition reactions.[1,2] In it, a 1,3-diene reacts with an olefin or acetylene dienophile to form an adduct with a six-membered ring. In the reaction two new σ bonds are formed at the expense of two π bonds of the starting material.[3−5] The usefulness of the DA reaction arises from its versatility and from its remarkable stereochemistry. By varying the nature of the diene and dienophile, many different types of carbocyclic structures can be built up. However, not all possibilities take place easily. Although the DA reaction between butadiene and ethylene must be forced to take place after 17 h at 165 °C and 900 atm, giving a yield of 78%, the presence of electron-releasing substituents in the diene and electron-withdrawing in the dienophile or vice versa can drastically accelerate the reaction.

The mechanism of the DA reaction has been controversial for some time.[6−8] The archetypal DA reaction of butadiene and ethylene is exothermic by 40 kcal/mol and has a reaction barrier of 27.5 kcal/mol.[9,10] It may occur via either a synchronous concerted mechanism along a pericyclic transition state or a stepwise mechanism involving the formation a diradical intermediate.[6−8] The butadiene + ethylene reaction however is not the typical case. In general, the DA reaction requires opposite electronic features in the substituents at the diene/dienophile pair for being reasonably fast. Recent studies point out that this type of substitution favors the charge transfer along an asynchronous mechanism.[11−16] Furthermore, the reaction mechanism changes progressively from a concerted, asynchronous one to a polar stepwise pathway with increasing ability of the dienophile to stabilize a negative charge.[17]

Several disubstituted acetylene derivatives as dimethyl acetylenedicarboxylate (DMAD) and acetylenedicarboxylic acid (ADA) have been used as activated dienophiles on DA reactions. They readily combine with all types of dienes to give 1,4-cyclohexadiene system. We have recently studied the mechanism of DA reactions of pyrrole and furan with the aforementioned acetylene derivatives.[18−22] The electron-rich character of pyrrole and furan heterocycles together with the large electron-poor character of DMAD and ADA make the reaction to take place along a stepwise mechanism with a large polar character.[20,21] The first step of the reaction corresponds to the nucleophilic attack of the C2 carbon atom of the heterocycle system to one conjugate position of the substituted acetylene to give a zwitterionic intermediate (see Scheme 1 and **TS1** in Figure 1). Moreover, for 2-substituted pyrroles, a competitive Michael reaction can

* To whom correspondence should be addressed. E-mail: domingo@utopia.uv.es.
† Instituto de Ciencia Molecular, Universidad de Valencia.
‡ Departamento de Química Orgánica, Universidad de Valencia.
§ Universidad de Chile.
|| Pontificia Universidad Católica de Chile.

10.1021/jp012603i CCC: $22.00
Published on Web 01/16/2002

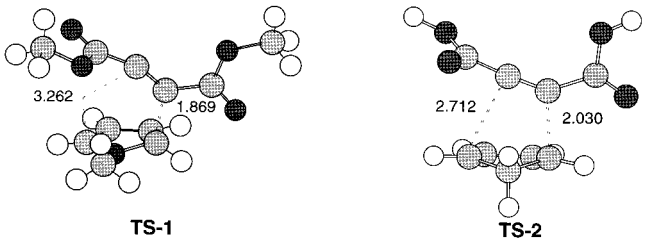

Figure 1. B3LYP/6-31G* Transition structures corresponding to the first step of the stepwise cycloaddition reaction between pyrrole and DMAD, **TS1**, and the concerted cycloaddition reaction between cyclopentadiene and ADA, **TS2**. The lengths of the C−C forming bonds involved in the reaction are given in angstroms.

SCHEME 1

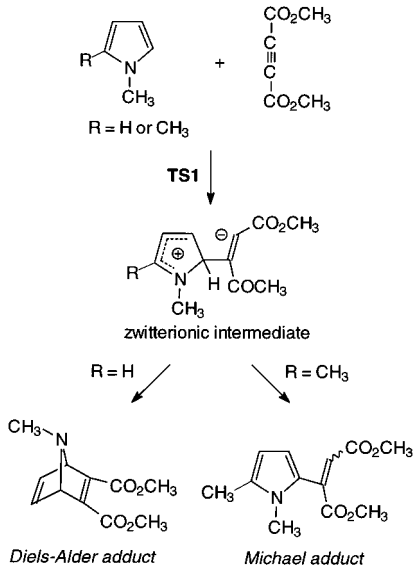

take place[20] which shares the aforementioned intermediate in agreement with a large polar character for these DA reactions (see Scheme 1).

The cycloaddition reaction of the low activated cyclopentadiene (Cp) with DMAD has been studied both experimentally[23] and theoretically.[24] The activation energy obtained for the reaction between Cp and ADA, as a model for DMAD, 14.1 kcal/mol (B3LYP/6-31G* level)[24] is in good agreement with the experiment, 13.8 kcal/mol.[23] This is significantly lower than that for the reaction of Cp with acetylene because of the electron-withdrawing effects of the two-carboxylate groups of DMAD.[24] The cycloaddition takes place along a concerted mechanism associated to a transition structure (TS) extremely asymmetric. The lengths of the two forming bonds are 2.030 and 2.712 Å, respectively (see **TS2** in Figure 1). This large asymmetry is obviously due to the electronic effect of the electron-withdrawing carboxylate substituents on the acetylene, which favor the C−C bond-formation at one of two conjugated positions of the doubly activated acetylene system.

The DA reaction between a low activated 1-vinyl-2-methylcyclohexene system and DMAD has been recently studied both experimentally and theoretically (see Scheme 2).[25] Along the cycloaddition an unique asynchronous concerted TS has been found at the low HF/STO-3G level. However, the lengths of the two forming bonds, 2.111 and 2.382 Å,[25] point out a low asynchronicity, $\Delta r = 0.2$, compared with that corresponding to the reaction between Cp and ADA, $\Delta r = 0.7$. These results indicate that both B3LYP/6-31G* and HF/STO-3G levels could be describing unlike bond-formation processes.

SCHEME 2

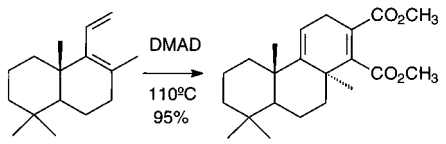

SCHEME 3: (a) Reaction Pathways for the Cycloadditions between 1,3-Butadiene, I, (*Z*)-1,3-Pentadiene, III, and 4-Methyl-1,3-pentadiene, IV, and DMAD. (b) Concerted Reaction Pathways for the Cycloadditions between (*E*)-1,3-Pentadiene, II, and DMAD

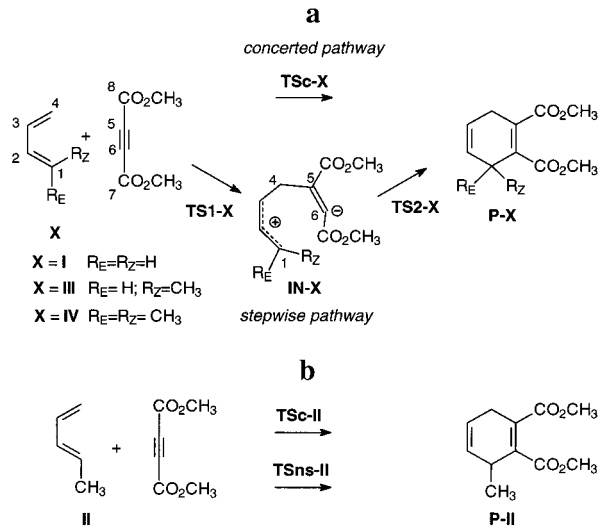

In view of these precedents, and as part of our research program devoted to the study of the molecular mechanism of the cycloaddition reactions that takes place via asynchronous bond-formation processes, a density functional theory (DFT) study for the reaction between four 1,3-butadiene (1,3-BDs) systems, 1,3-butadiene **I**, (*E*)-1,3-pentadiene **II**, (*Z*)-1,3-pentadiene **III**, and 4-methyl-1,3-pentadiene **IV**, and DMAD is now presented (see Scheme 3). The purpose of this study is to contribute to a better understanding of the features of the diene and dienophile responsible for the concerted and stepwise mechanism of these cycloadditions.

Global and Local Properties

Global electronic indexes, as defined within the DFT of Parr, Pearson, and Yang[26,27] are useful tools to understand the reactivity of molecules in their ground states. For instance, the electronic chemical potential μ describing the changes in electronic energy with respect to the number of electrons is usually associated with the charge-transfer ability of the system in its ground-state geometry. It has been given a very simple operational formula in terms of the one electron energies of the frontier molecular orbital HOMO and LUMO, ϵ_H and ϵ_L, as

$$\mu \approx \frac{\epsilon_H + \epsilon_L}{2} \tag{1}$$

Besides this index, it is also possible to give a quantitative representation to the chemical hardness concept introduced by Pearson,[28] which may be represented as[26]

$$\eta \approx \epsilon_L - \epsilon_H \tag{2}$$

Recently, Parr et al.[29] have introduced a new and useful definition of global electrophilicity, which measures the stabi-

lization in energy when the system acquires an additional electronic charge ΔN from the environment. The electrophilicity power has been given the following simple expression:[29]

$$\omega = \frac{\mu^2}{2\eta} \tag{3}$$

in terms of the electronic chemical potential μ and the chemical hardness η, defined in eqs 1 and 2.

Local (regional) quantities on the other hand, are useful descriptors of reactivity toward electrophilic, nucleophilic, and radical attacks.[26,30−32] Their variations upon external stimuli, as for instance the change in the number of electrons induced by chemical substitutions, give relevant information about the electrophilic/nucleophilic activation at a given site upon interaction with the environment (reagents, solvent effects, etc.).[33] Local activation in regional softness may be expressed as

$$\Delta s_k^\alpha = f_k^{\alpha,O}\Delta S + S\Delta f_k^\alpha \tag{4}$$

in terms of the nucleophilic and electrophilic Fukui functions f_k^α where $\alpha = +$ and $-$, respectively. ΔS is the variation in global softness from the reactant ground state to the transition state (activation softness), and $\Delta f_k^\alpha = f_k^\alpha(TS) - f_k^{\alpha,o}$. $f_k^{\alpha,o}$ is the Fukui function evaluated at the ground state of molecules. Expression 4 describes the activation in local softness to an activated complex structure as for instance the TS structure. It is obtained by performing a first-order variation in the local softness defined by $s(\mathbf{r}) = f(\mathbf{r})\, S$.

Computational Details

All calculations were carried out with the Gaussian 98 suite of programs.[34] Previous theoretical studies of Diels−Alder reactions have indicated that the activation energies calculated at the HF level are too large, whereas MP2 calculations tend to underestimate them. However, energy calculations for stationary points using MP3/6-31G* are in accord with experimental values.[14,16,35] Recently, DFT calculations[26,36] using the B3LYP[37,38] hybrid functional together with the 6-31G* basis set[39] have been shown to be in good agreement with experimental activation energy values[40−44] and to give a similar potential energy barriers to that obtained using time-consuming MP3 calculations.[45,46] Consequently, all stationary points were optimized at the B3LYP/6-31G* level, to obtain accurate energies for a correct characterization of the PES. The geometry optimizations were carried out using the Berny analytical gradient optimization method.[47,48] The stationary points were characterized by frequency calculations in order to verify that minima and transition structures have zero and one imaginary frequency, respectively. Zero-point vibrational energies (ZPVEs) have been computed at DFT levels; the ZPVEs have been scaled by 0.98.[49] The transition vectors,[50] i.e., the eigenvector associated to the unique negative eigenvalue of the force constants matrix, have also been characterized. The intrinsic reaction coordinate (IRC)[51] paths were traced in order to check the energy profiles connecting each transition structure to the two associated minima of the proposed mechanism, by using the second-order González−Schlegel integration method.[52,53] Several conformations related to the rotation around the C−C single bond involving the carboxylate groups have been considered. Those presented here correspond to the most stable ones. Optimized geometries of all stationary points on PES are available from the authors.

The electronic structure of the stationary points were analyzed using the natural bond orbital (NBO) method.[54,55] Because some reactive channels present very asynchronous TSs, diradical structures could in principle be involved. This has been ruled out by checking the wave functions of all TSs with unrestricted DFT theory. UB3LYP/6-31G* calculations, using the keyword STABLE in Gaussian 98, predict the same TSs as the one obtained from the restricted B3LYP/6-31G* calculations, thereby indicating that the restricted DFT solutions are stable.[56,57]

Most of the chemical reactions are performed in solution, and therefore, solvent effects could yield valuable information about the reaction mechanism. The need to increase our knowledge about interactions between solvent and solute remains as a crucial aspect of chemical reactivity. Solvent effects have been considered by B3LYP/6-31G* optimizations of stationary points using a relatively simple self-consistent reaction field (SCRF)[58,59] based on the polarizable continuum model (PCM) developed by Tomasi's group.[60−62] One of the solvents used in the experimental works is toluene. Therefore, we have used a dielectric constant $\epsilon = 2.38$ to mimic this solvent at 298.0 K.

Electrophilic and nucleophilic Fukui functions (FFs) condensed to atoms have been evaluated from a single-point calculations performed at the ground state of molecules at the same level of theory, using a method described elsewhere.[63,64] This method evaluates FFs using the coefficients of the frontier molecular orbitals (FMOs) involved in the reaction and the overlap matrix. Global softness values needed to convert regional FFs into regional softness were obtained from the one electron energies of the FMOs HOMO and LUMO as $S \approx 1/(\epsilon_L - \epsilon_H)$. The global electrophilicity power was evaluated using eq 3 with the electronic chemical potential and chemical hardness given by eqs 1 and 2.

Results and Discussion

(a) Energies. An analysis of the PESs for the cycloaddition reactions of 1,3-butadiene **I**, (Z)-1,3-pentadiene **III**, and 1-methyl-1,3-pentadiene **IV** with DMAD shows that these reactions can take place along two competitive reactive channels corresponding to the concerted and the stepwise bond-formation processes. Although along the concerted pathways the two σ bonds are simultaneously formed although not necessarily in a synchronous way, at the stepwise pathways, a σ bond is first formed along the nucleophilic attack of 1,3-BD to DMAD to give an acyclic intermediate. Thus, three TSs, **TSc-X**, **TS1-X**, and **TS2-X**, an intermediate, **IN-X**, and a cycloadduct, **P−X**, (**X** = **I**, **III** and **IV**), have been characterize. **TSc-X** corresponds to the concerted mechanism, whereas **TS1-X** and **TS2-X** are the TSs associated to the first and second step of the stepwise mechanism, respectively (see Scheme 3a). A quite different result is found for the cycloaddition using (*E*)-1,3-pentadiene **II**. Now the initial nucleophilic attack of **II** to DMAD is followed by the concomitant ring closure, and in consequence, an unique highly asynchronous TS, **TSns-II**, is found along the cycloaddition reaction (see Scheme 3b). The stationary points corresponding to these cycloaddition reactions are shown in Scheme 3, together with atom numbering. The B3LYP/6-31G* total and relative energies are summarized in Table 1. The geometries of the TSs are presented in Figures 2 and 3.

For these acyclic 1,3-BDs, two twisted conformations are possible corresponding to the s-cis and s-trans arrangement of the 1,3-butadiene system. The s-trans conformations are between 3.5 and 3.8 less energetic than the s-cis ones because the hindrance between the C1 and C4 methylene groups at the s-cis arrangement. However, the low rotational barrier around the C2−C3 single bond allows at the experimental conditions the easy equilibrium between both conformers.

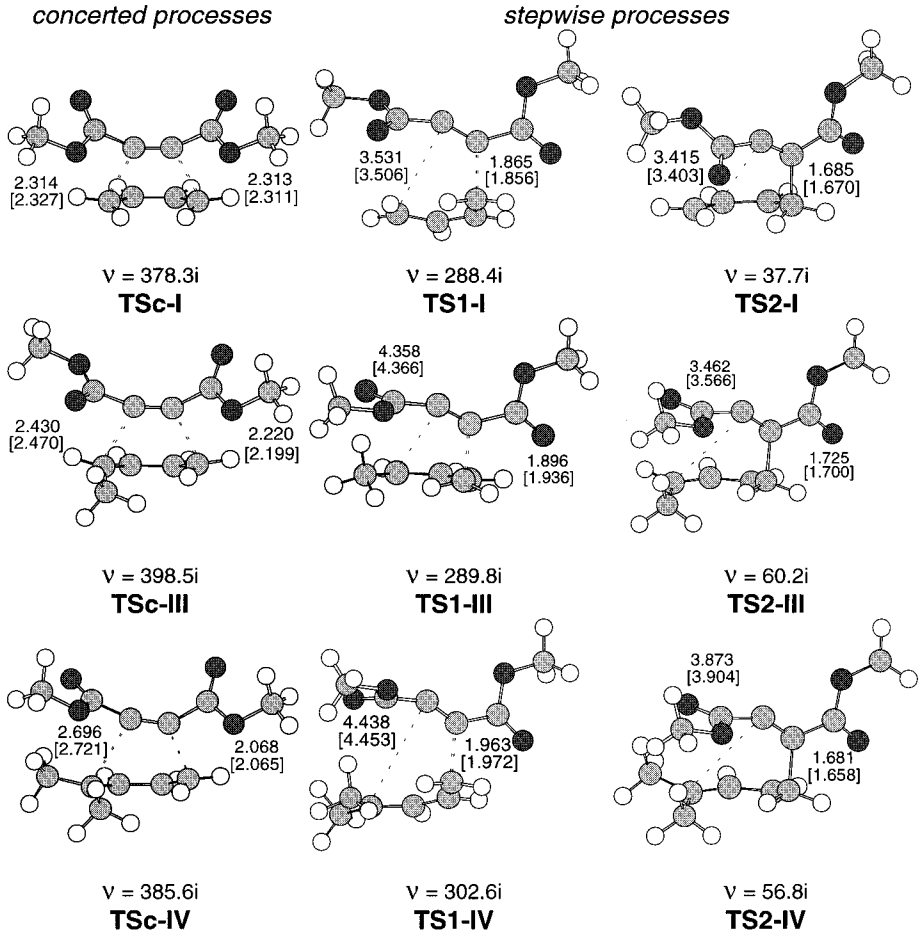

Figure 2. Transition structures corresponding to the concerted, **TSc-X**, and stepwise, **TS1-X** and **TS2-X**, reaction pathways corresponding to the cycloaddition reactions between the 1,3-BDs **I**, **III**, and **IV** and DMAD. The values of the lengths of the bonds directly involved in the reaction obtained at the B3LYP/6-31G* and B3LYP/6-31G* in toluene (numbers in brackets) are given in angstroms. The unique imaginary frequencies, ν in cm^{-1}, are also given.

TABLE 1: Total Energies[a,b] (au) and Relative Energies[c] (kcal/mol, in Parentheses) for the Stationary Points Corresponding to the Cycloaddition Reaction between the 1,3-Butadienes I−IV and DMAD

	I		**II**		**III**		**IV**	
s-trans **X**	−155.904556		−195.197443		−195.194422		−234.486720	
s-cis **X**	−155.910072	(3.5)	−195.202983	(3.5)	−195.200327	(3.7)	−234.492865	(3.9)
TSc-X	−688.842581	(20.1)	−728.134817	(20.6)	−728.125892	(24.5)	−767.416821	(25.5)
TSns-X			−728.137823	(18.7)				
TS1-X	−688.840985	(21.1)			−728.130184	(21.8)	−767.423947	(21.0)
IN-X	−688.840667	(21.3)			−728.130400	(21.7)	−767.424926	(20.4)
TS2-X	−688.840707	(21.3)			−728.125343	(24.8)	−767.421393	(22.6)
P−X	−688.967214	(−58.1)	−728.253281	(−53.8)	−728.253281	(−55.4)	−767.539677	(−51.6)

[a] Including ZPVEs. [b] For DMAD −532.964599 ua. [c] Relative to s-trans **X** + DMAD.

The potential energy barriers (PEBs) associated to the cycloadditions between these 1,3-DBs, **I** to **IV**, and DMAD are within the range of 18.7 and 24.5 kcal/mol.[65] The PEB for the reaction between 1,3-butadiene **I** and DMAD, 20.1 kcal/mol, is lower than that for the reaction between 1,3-butadiene and ethylene, 24.8 kcal/mol,[24] because of the electron-withdrawing effects of the carboxylate groups of DMAD. These cycloadditions are very exothermic processes, in the range of −52 to −58 kcal/mol.

An analysis of the relative energies presented in Table 1 shows a relationship between the relative values of the PEBs and the methyl substitution on the butadiene system. The PEB for the cycloaddition between (*E*)-1,3-pentadiene, **II**, is 1.4 kcal/mol less energetic than that for the reaction with 1,3-butadiene, **I**, whereas the reaction with (*Z*)-1,3-pentadiene, **III**, and 4-methyl-1,3-pentadiene, **IV**, are 4.4 and 2.5 kcal/mol more energetic than that for **I** (see Table 1).

To better understand these energetic results, the substitution effects on the barriers may be interpreted in terms of two opposite contributions: the first one is a favorable electronic effect associated to the substitution of an hydrogen atom by an electron-releasing methyl group, which increases the nucleophilicity of the butadiene system (see section e). The second one is associated to the hindrance that appears along the bond-formation process because of the presence of a bulky methyl group instead of a small hydrogen atom. Thus, although the substitution of the *E* hydrogen atom by a methyl group decreases the barrier in ca. 1.4 kcal/mol, the inclusion of a second methyl group increases it in ca. 2.5 kcal/mol. These results indicate that, for the *E* substitution, the hindrance promoted by the methyl

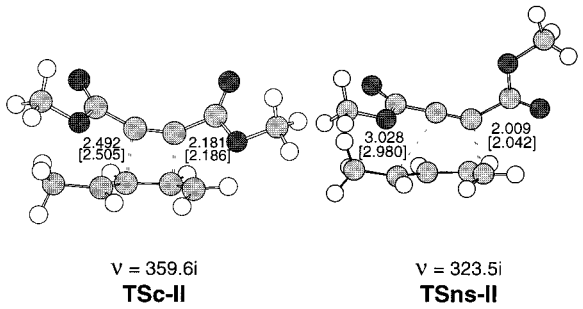

Figure 3. Transition structures of the concerted reaction pathways corresponding to the cycloaddition reactions between the (*E*)-1,3-pentadienes **II** and DMAD. The values of the lengths of the bonds directly involved in the reaction obtained at the B3LYP/6-31G* and B3LYP/6-31G* in toluene (numbers in brackets) are given in angstroms. The unique imaginary frequencies, ν in cm^{-1}, are also given.

group is balanced by the electron-releasing effect of this group, and therefore, the reaction is accelerated by electronic arguments. However, the inclusion of the second methyl group makes the process more unfavorable because the hindrance for the approach of DMAD to **IV**.

Moreover, the *E* and *Z* substitutions on the 1,3-butadiene system has a different role on the barrier heights. At (*Z*)-1,3-pentadiene **III**, the hindrance that appears between the C1 methyl substituent and the C4 methylene group at the s-cis conformation makes that of the C1−C2−C3−C4 dihedral angle be twisted in order to minimize the unfavorable interactions. However, along the cycloaddition reaction the 1,3-butadiene system must be in a planar arrangement in order to perform a larger overlap between the C2 and C3 carbon atoms. This demand decreases the C1−C2−C3−C4 dihedral angle, increasing the hindrance and the energy of the TS. In consequence, the cycloaddition with **III** presents the more defavorable barrier. A similar behavior is found at the 1,3-BD **IV**.

Even more interesting conclusions can be obtained if the two competitive mechanisms, the concerted and the stepwise ones, are considered. For instance, for the reaction between 1,3-BD **I** and DMAD, the concerted **TSc**−**I** is 1.0 kcal/mol more favorable than the **TS1**−**I** corresponding to the first step of the stepwise mechanism. However, the inclusion of the *E* methyl group in the 1,3-BD system changes the relative energies; now, the highly asynchronous **TSns-II** is 1.9 kcal/mol more favorable than the concerted **TSc**−**II**. A quite different result is obtained with the *Z* methyl substitution. Although **TS1**−**III** is 2.7 kcal/mol more favorable than **TSc**−**III**, the hindrance that appear along the cyclization process makes the second as the rate-determining step, and now the concerted process is favored by only 0.3 kcal/mol. These behaviors can be explained by two opposite factor: the increase of the nucleophilic character of 1,3-BDs with the presence of the electron-releasing methyl groups that favors the stepwise processes and a destabilization of the corresponding TSs because the hindrance imposed by the larger methyl substituent.

These features allow us to explain the deceleration found at the 4-methyl-1,3-pentadiene **IV**. Along the concerted process, the presence of the two methyl groups arises **TSc**−**IV** 5.0 kcal/mol above **TS1**−**IV** corresponding to the stepwise process. However, along the stepwise process, the hindrance has a more remarkable effect at the cyclization step, and now the second step via **TS2**−**IV** is the rate-determining step. The presence of two electron-releasing methyl groups at **IV** however makes the stepwise mechanism 2.9 kcal/mol more favorable that the concerted one.

(b) Geometries and Frequency Analysis. The lengths of the C1−C6 and C4−C5 forming bond at the TSs associated to the concerted processes are 2.314 and 2.314 Å for **TSc**−**I**; 2.492 and 2.181 Å for **TSc**−**II**; 2.430 and 2.220 Å for **TSc**−**III**; and 2.696 and 2.068 Å for **TSc**−**IV**, respectively (see Figures 2 and 3). These bond lengths indicate that, although **TSc**−**I** corresponds to a synchronous process, **TSc**−**II, TSc**−**III**, and **TSc**−**IV** correspond to asynchronous processes where the C4−C5 bond is formed in a larger extent than the C1−C6 one. Both (*E*) and (*Z*) isomers of 1,3-pentadiene present similar asynchronicity. For the asynchronous processes, the larger C1−C6 bond length can be rationalized as a consequence of the hindrance that appears between the methyl groups present on the C1 position of the 1,3-BD systems and the C6 carboxylate group of DMAD along the C1−C6 bond-formation. Therefore, the dimethyl substituted butadiene **IV** presents the largest asynchronicity, the C4−C5 bond length being 2.696 Å. Further, the presence of the electron-releasing methyl groups at the C1 position breaks the symmetry of 1,2-butadiene thereby increasing the nucleophilic character at C4 position.[66] Therefore, there is a shortening of the C4−C5 lengths induced by C1 methyl substitution.

The values of the unique imaginary frequency of the TSs corresponding to the concerted bond-formation processes are 378i cm^{-1} for **TSc**−**I**, 360i cm^{-1} for **TSc**−**II**, 399i cm^{-1} for **TSc**−**III** and 386i cm^{-1} for **TSc**−**IV**. The analysis of the atomic motions along these vibrational frequencies indicates that these TSs are mainly associated to the motion of the C1, C4, C5, and C6 carbon atoms along the C1−C6 and C4−C5 bond-formation processes. Finally, the analysis of the transition vector associated to these TSs shows a larger participation of the C1−C6 and C4−C5 lengths in agreement with concerted bond-formation processes. (The main components of the transition vector of the highly asynchronous **TSc**−**IV** are associated with the C1−C6 (0.423) and C4−C5 (0.778) bond lengths.)

For the TSs corresponding to the first step of the stepwise processes, the lengths of the C4−C5 bond are 1.865 Å for **TS1**−**I**, 1.896 Å for **TS1**−**III**, and 1.963 Å for **TS1**−**VI**, whereas the distance between the C1 and C6 carbon atoms becomes 3.531 Å for **TS1**−**I**, 4.358 Å for **TS1**−**III**, and 4.438 Å for **TS1**−**VI**. At these TSs, the C1−C6 distance increases with the substitution at the C1 position. The C4−C5 bond lengths at the corresponding intermediates are ca. 1.7 Å, whereas the C1−C6 distance remain very large, in the range of 3.6−4.4 Å. Finally, at the TSs corresponding to the second step, the length of the C1−C6 bonds are 3.415 Å for **TS2**−**I**, 3.462 Å for **TS2**−**III**, and 3.873 Å for **TS2**−**IV**.

For the **TSns-II**, the length of the C4−C5 bond is 2.009 Å, whereas the distance between the C1 and C6 carbon atoms become 3.028 Å. These lengths indicate that this TS corresponds to an highly asynchronous bond-formation process.

The values of the unique imaginary frequency of the TSs corresponding to the first step of the stepwise processes are 288i cm^{-1} for **TS1**−**I**, 290i cm^{-1} for **TS1**−**III**, and 303i cm^{-1} for **TS1**−**IV**. For **TSns-II**, this value is 324 cm^{-1}. These values are lower than those corresponding to the concerted processes. The analysis of the atomic motion along these vibrational frequencies indicates that these TSs are mainly associated to the motion of the C4 and C5 carbon atoms along the C4−C5 bond-formation processes. The motion of the C1 and C6 carbon atoms is negligible. For the TSs corresponding to the second step, the values of the unique imaginary frequency lies between 38 and 60 cm^{-1}. The analysis of the atomic motion along these vibrational frequencies shows that these TSs are mainly associ-

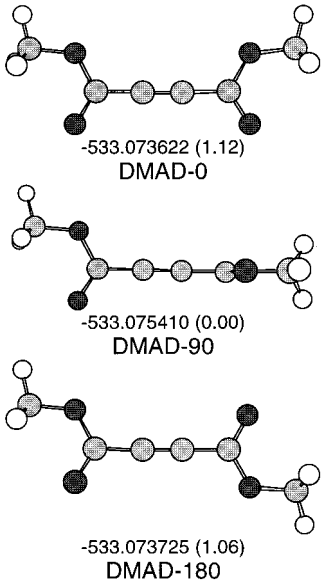

Figure 4. Conformations of DMAD. The total (in au) and the relative energies (in kcal/mol, in parentheses; relative to DMAD-90) are given also.

ated to the C4−C5 single bond rotation at the corresponding intermediates, which allows the approach of the C1 and C6 centers.

A comparison of the geometries corresponding to the concerted TSs, **TSc-X**, and those corresponding to the first step of the stepwise mechanism, **TS1-X** and **TSns-II**, reveals two significant differences. The first one is related to the value of the C8−C5−C6 bond angles and the C8−C5−C6−C7 dihedral angles, and the second one is related to the different arrangement of the two-carboxylate groups belonging to the DMAD moiety.

At the TSs, the C5, C6, C7, and C8 carbon atoms are in same plane due to the sp or sp^2 hibridization of the C5 and C6 atoms belonging to the acetylene system. However, although along the concerted processes the simultaneously bond-formation demand a cis arrangement for the two-carboxylate groups, the corresponding C8−C5−C6−C7 dihedral angle at **TSc-X** is ca. 0°; along the stepwise processes, these groups adopt a trans arrangement with a corresponding dihedral angle of ca. 180° at **TS1-X**. This trans arrangement minimize the electronic repulsion between the C4−C5 forming bond and the charge that is transferred to the C6 carbon atom. The linear arrangement of the C5−C6−C7 carbon atoms at the highly asynchronous **TSns-II** indicates that the C6 carbon atom remains sp.

Furthermore, the two-carboxylate groups belonging to the DMAD adopt different arrangements at these TSs. Although at the concerted transition states the two-carboxylate groups are in a nearly planar arrangement, along the stepwise processes, they are in a perpendicular arrangement. To explain this behavior, we propose to consider first the molecular structure of DMAD. Because of the free rotation of the two carboxylate groups of DMAD around the C5−C8 and C6−C7 single bonds, this acetylene derivative can adopt three different conformations, namely, the DMAD-0, DMAD-90, and DMAD-180 structures shown in Figure 4. They are related to the dihedral angle between the two C−O double bonds of the two-carboxylate groups. For instance, in DMAD-0 and DMAD-180 structures, the two C−O double bonds are in a planar arrangement forming a dihedral angle of 0° and 180°, respectively, whereas in DMAD-90, the two C−O double bonds are in a perpendicular arrangement, forming a dihedral angle of 90° (see Figure 4). The relative energy of these conformations falls in a narrow range of 1.2 kcal/mol, and therefore, it may be concluded that there is a free rotation around the C−C acetylene axis.[24]

These different arrangements however have unlike electronic features with respect to the two orthogonal π systems of the acetylene framework. Although in the planar arrangement, DMAD-0 and DMAD-180, both carboxylate groups are conjugated to one π system, at the perpendicular conformation DMAD-90, each carboxylate group is conjugated to one of the two π systems of the triple C−C bond of DMAD. Thus, along the concerted bond-formation processes, **TSc-X**, the planar arrangement of the two electron-withdrawing carboxylate groups simultaneously activates the π acetylene system involved at the concerted bond-formation process. However, along the nucleophilic attack of the C4 carbon atom of 1,3-BDs to the C5 conjugated position of DMAD the charge transferred is being located at the C6 carbon atom. The perpendicular arrangement favors both bond-formation and charge transfer by a large polarization of the acetylene system when each carboxylate group is conjugated with a different π system of acetylene, **TSns-II** and **TS1-X**. Site activation induced by the different conformations of the carboxylate groups in DMAD will be discussed in more detail in section e below.

(c) Bond Order and Charge Analysis. The extent of bond-formation or bond breaking along a reaction pathway is provided by the concept of bond order (BO). This theoretical tool has been used to study the molecular mechanism of chemical reactions. To follow the nature of these processes, the Wiberg bond indexes[67] have been computed by using the NBO population analysis as implemented in Gaussian 98. The results are included in Table 2.

For the TSs corresponding to the concerted bond-formation processes, the values of the BO for the C4−C5 and C1−C6 forming bonds are ca. 0.27 and 0.27 for **TSc−I**, 0.34 and 0.22 for **TSc−II**, 0.32 and 0.23 for **TSc−III**, and 0.41 and 0.17 for **TSc−IV**, respectively. Although **TSc−I**, corresponds to a synchronous TS, the others are asynchronous TSs. These BO values show an increase of the asynchronicity with methyl substitution at the C1 position. Moreover, both (*Z*) and (*E*) isomers of the 1,3-pentadiene have similar asynchronicity, showing a like bond-formation pattern. It is interesting to remark that along the concerted processes the sum of the C4−C5 and C1−C6 bond order values remain around 0.55. Thus, at the most asynchronous **TSc−IV** channel, the lack of covalent interactions along the C1−C6 bond-formation measured by the bond order value is counterbalanced by a larger covalent interaction along the C4−C5 bond formation.

For the TSs corresponding to the first step of the stepwise processes, the values of the BO for the C4−C5 forming bond are 0.53, 0.52, and 0.49, for **TS1−I**, **TS1−III**, and **TS1−IV**, respectively. At these TSs, the BO values between the C1 and C6 are 0.1. At the corresponding intermediates, the values of the BO for the C4−C5 bond are ca. 0.7, whereas the values of the BO for the C5−C6 bond, ca. 2.0, suggest the formation of the C5−C6 double bond from the triple one present in DMAD.

For **TSns-II**, the values of the BO for the C4−C5 and C1−C6 forming bonds, 0.44 and 0.14, respectively, indicate that this TS corresponds to an highly asynchronous bond-formation process.

The natural population analysis[54] allows evaluating the charge transferred along these cycloaddition processes.[57] The atomic charges have been partitioned between the donor 1,3-BDs and the acceptor DMAD (see Table 2). The values of the charge transferred from the 1,3-BDs to DMAD along the concerted processes are 0.16 e at **TSc−I**, 0.18 e at **TSc−II**, 0.19 e at

TABLE 2: Wiber Index (BO) and Charge Transfer (QT, in au) for the Concerted and Stepwise Mechanisms of the Cycloaddition Reaction between the 1,3-Butadienes I, II, and III and DMAD

	BO	QT		BO	QT		BO	QT		BO	QT	
TSc−I	0.27	0.16	**TSc−II**	0.34	0.18	**TSc−III**	0.32	0.19	**TSc−IV**	0.41	0.22	C4−C5
	0.27			0.22			0.23			0.17		C1−C6
TS1−I	0.53	0.22				**TS1−III**	0.52	0.25	**TS1−IV**	0.49	0.27	C4−C5
	0.10						0.10			0.08		C1−C6
IN−I	0.70					**IN−III**	0.75		**IN−IV**	0.77		C4−C5
	0.15						0.14			0.13		C1−C6
			TSns-II	0.44	0.23							C4−C5
				0.14								C1−C6

TABLE 3: Total Energies[a,b] (au) and Relative Energies[c] (kcal/mol, in Parentheses) for the Stationary Points Corresponding to the Cycloaddition Reaction between the 1,3-Butadienes I−IV and DMAD in Toluene

	I		II		III		IV	
s-trans **X**	−155.910528		−195.203522		−195.200837		−234.493404	
TSc-X	−688.846228	(19.8)	−728.138545	(20.3)	−728.129195	(24.4)	−767.420485	(25.2)
TSns-X			−728.140635	(18.9)				
TS1-X	−688.844259	(21.1)			−728.133330	(21.8)	−767.427130	(21.1)
IN-X	−688.844088	(21.2)			−728.134066	(21.4)	−767.429066	(19.9)
TS2-X	−688.844159	(21.1)			−728.129363	(24.3)	−767.425435	(22.1)
P−X	−688.970454	(−58.1)	−728.256341	(−53.7)	−728.256341	(−55.3)	−767.542320	(−51.2)

[a] Including ZPVEs. [b] For DMAD −532.967300 ua. [c] Relative to s-trans **X** + DMAD.

TSc−III, and 0.22 e at **TSc−IV**, whereas these values at the TSs corresponding to the first step of the stepwise mechanism become 0.22 e at **TS1−I**, 0.25 e at **TS1−III**, and 0.27 e at **TS1−IV**. The larger values found at the TSs corresponding to the stepwise mechanisms relative to those for the concerted one agree with a larger polar character for the former. This behavior is a consequence of the perpendicular arrangement of two-carboxylate groups that favor the charge transfer by a large polarization of the acetylene system. Moreover, these values also show an increase of the charge transfer induced by methyl substitution, in agreement with the lowering in global electrophilicity of these substituted 1,3-BDs (see section e), and the decrease of the barrier associated to the cycloaddition process. Finally, the charge transferred at the highly asynchronous concerted **TSns-II**, 0.23 e, is similar than that found at **TS1−III**.

An analysis of the results indicates that although **TSc−II** and **TSns-II** correspond to concerted reactions because they take place in a single kinetic step, they describe unlike bond-formation processes. Thus, whereas **TSc−II** corresponds to a *concerted asynchronous reaction* in which all of the forming and breaking bond processes take place at the same time although not necessarily via a synchronous fashion, **TSns-II** corresponds to a *two-stage reaction* which is concerted but not synchronous.[68] At this process, some of the changes in bonding take place in the first half of the reaction, between the reactants and TS, whereas the rest takes place in the second half of the reactions, between TS and the products.[69] Thus, the highly asynchronous **TSns-II** corresponds to a polar process similar to that described by **TS1-x** where the cycloadduct is subsequently formed after the nucleophilic attack of **II** to DMAD because the nonexistence of a significant barrier for the cyclization process.

(d) Solvent Effects. Solvent effects on cycloaddition reactions are well-known and have received considerable attention, especially in the past few years. Solvent effects have been introduced using the PCM method of Tomasi's group.[60−62] Table 3 reports the total and relative energies obtained with the inclusion of solvent effects, whereas the geometrical parameters are included in Figures 2 and 3.

With the inclusion of solvation, the TS and intermediate structures are stabilized by about 2−3 kcal/mol. However, if we consider that the reactants are stabilized 2.0 kcal/mol, we found a poor global solvent effect in these cycloadditions. These results are due to the effective delocalization of the charge transferred along the nucleophilic attack of these 1,3-BDs to DMAD[20,21] and also due to the low polarity of toluene.

TABLE 4: Global Properties for Acetylene Derivative and Different Substituted Butadienes[a]

molecule	μ	η	ω
DMAD-0	−0.1831	0.2007	2.27
DMAD-90	−0.1717	0.2345	1.71
1,3-butadiene (**I**)	−0.1270	0.2083	1.05
(*E*)-1,3-pentadiene (**II**)	−0.1182	0.2037	0.93
(*Z*)-1,3-pentadiene (**III**)	−0.1190	0.2089	0.92
4-methyl-1,3-pentadiene (**IV**)	−0.1137	0.2048	0.86

[a] Electronic chemical potential and chemical hardness values are in au; electrophilicity power values are in eV.

Finally, a comparison of the geometrical parameters of the TSs given in Figures 2 and 3 shows that the inclusion of solvent effects on the geometry optimization does not modify substantially the geometries obtained in a vacuum. In consequence, these competitive concerted and stepwise mechanisms remain even with the inclusion of solvent effect.

(e) Global Electrophilicity Analysis and Site Activation Model. These cycloaddition reactions have been also analyzed using local and global indexes defined in the context of DFT. In Table 4 are displayed the static global properties, electronic chemical potential μ, chemical hardness η, and global electrophilicity ω, defined in eqs 1−3, for the 1,3-BDs **I**, **II**, **III**, and **IV** and dimethyl acetylenedicarboxylate in their planar DMAD-0 and perpendicular DMAD-90 conformations. The DMAD-90 conformation has lower energy and higher hardness than the DMAD-0 one, in agreement with the maximum hardness principle.[63] This enhancement in chemical hardness contributes to the lowering in global electrophilicity power from $\omega = 2.27$ eV in the DMAD-0 conformation to $\omega = 1.71$ eV in the DMAD-90 structure. Within the 1,3-BDs subseries, increasing substitution by methyl groups at position 1 results in a slight enhancement in chemical hardness, that entails a lowering in global electrophilicity from 1.05 eV in 1,3-butadiene **I** to 0.86 eV in 4-methyl-1,3-pentadiene **IV**. Moreover, both (*Z*) and (*E*) isomers of 1,3-pentadiene present a similar global electrophilicity. On the basis of the global electrophilicity power, DMAD in both conformations is expected to behave as electrophile with

TABLE 5: Local and Activation Properties of Planar and Perpendicular Conformations of DMAD with CN^- as a Model Nucleophile[a]

entry		site (k)	f_k^+	f_k^-	s_k^+	s_k^-	Δf_k^-	ΔS_k^-
i	DMAD-0	C6	0.1844	0.2009	0.9183	1.0005	0.0	0.0
		C5	0.1844	0.2009	0.9183	1.0005	0.0	0.0
ii	DMAD-90	C6	0.1996	0.1477	0.8502	0.6292	−0.0532	−0.3713
		C5	0.1996	0.1477	0.8502	0.6292	−0.0532	−0.3713
iii	DMAD-0 + CN^-	C6	0.0483	0.4352	0.3043	2.7417	0.2343	1.7412
		C5	0.1677	0.0269	1.0565	0.1695	−0.1740	−0.8310
iv	DMAD-90 + CN^-	C6	0.3179	0.4727	1.9583	2.9118	0.3250	2.2826
		C5	0.0825	0.0288	0.5082	0.1774	−0.1189	−0.4518
v	**TSc−I**	C6	0.1585	0.0442	0.8353	0.2329	−0.1567	−0.7676
		C5	0.1585	0.0442	0.8353	0.2329	−0.1567	−0.7676
vi	**TS1−I**	C6	0.2030	0.3388	1.8798	3.1373	0.1911	2.5081
		C5	0.0664	0.0374	0.6152	0.3463	−0.1103	−0.2829

[a] Activation properties of **TSc−I** and **TS1-I** have been also included. Global and local softness values are in au; electrophilicity values are in eV. See the text for details.

respect to these 1,3-BDs. Note that the electronic chemical potential of DMAD in any of the two conformations is lower than the electronic chemical potential of these 1,3-BDs, thereby indicating that, upon interaction, the charge flux will be from 1,3-BDs to DMAD, in agreement with the charge-transfer analysis give at the section c.

To perform the site activation analysis for the interaction of DMAD with these 1,3-BDs, we evaluated the local properties f_k^+, f_k^-, s_k^+, and s_k^- for models of site activation with reference to two possible conformations of DMAD electrophile which are depicted in Table 5. The entry i is the reference state for the activation properties induced by rotation around the principal C5−C6 axis. Local properties at C5 and C6 for the perpendicular conformation are depicted in entry ii of Table 5. It may be seen that rotation about C5−C6 axis marginally deactivates both sites toward electrophilic attacks, on the basis of the variation of the nucleophilic Fukui functions. Variations in local softness contain, apart of the variations in the Fukui functions, the global effect encompassed in the variations in global softness (see eq 4). The deactivation in nucleophilic softness is therefore driven by global changes (see Table 4).

A comparison of the global parameters for both conformation of DMAD with the analysis of the charge transfer at the TSs corresponding to the concerted and stepwise process indicates that the global and local properties obtained for the isolated DMAD are not adequate to explain its marked electrophilic character. In consequence, we have chosen to study the local response to the attack by the model nucleophile CN^- to DMAD. This perturbing model reagent was located at 2.1 Å of the C5 site, and its orientation with respect to DMAD as well as the internal parameters of the substrate were completely relaxed by a restricted geometry optimization (see Figure 5). Entry iii of Table 5 contains the activation parameters for the planar DMAD-0 perturbed by the model nucleophile CN^-. It may be seen that upon perturbation at C5 the β carbon (C6) is nucleophilically activated ($\Delta f_{C6}^- > 0$) and becomes a softer site for an electrophilic attack (i.e., the site becomes more nucleophilic and softer with reference to the planar isolated structure). The local contribution to the deactivation at site C5 may be traced to the direct interaction with the model nucleophile CN^-, whereas electrophilic deactivation at site C6 may also arise from an extra charge accumulation at that site.

Activation of the DMAD-90 conformation models the interaction pattern at the TS structures for the stepwise mechanism, **TS1-X**. In this case, activation properties are defined with reference isolated DMAD-90. The activation parameters are shown in entry iv of Table 5. The variations in the nucleophilic Fukui function at site C6 are activating as well as its local softness. Increase in local softness at C6 may be explained by strong global activation ($\Delta S = 1.9$ au). Note that in the perpendicular conformation the complex DMAD-CN^- becomes significantly more activated and softer at C6, as compared to the planar perturbed complex. The local enhancement in nucleophilicity at the β position (C6) in perpendicular conformation, as measured by Δf_{C6}^-, may be attributed to a local response at this site that reflect a more efficient electronic charge accumulation, probably favored by the interaction of the π^* orbitals of the two perpendicular carboxylate groups with the two orthogonal π system of acetylene. Variations in local softness cooperatively contribute to favor the ionic interaction found at the TS structure discussed in the precedent sections. It is interesting to note that even though the DMAD-90 displays a lower global electrophilicity than the DMAD-0 one the former shows a greater activation at the nucleophilic site than the second one. This behavior can be probably due to the favorable interaction of both perpendicular carboxylate groups with the two orthogonal π systems of the acetylene.

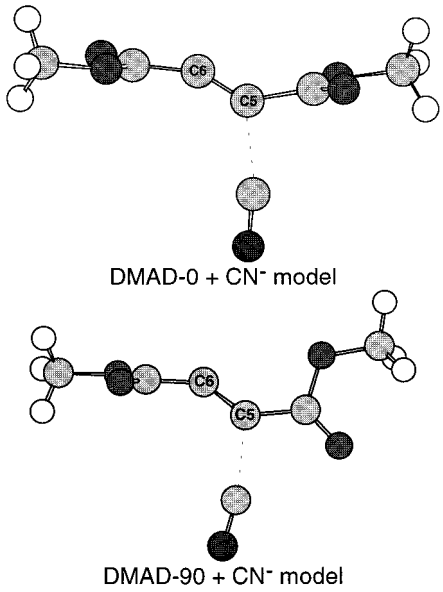

Figure 5. Computational models for the nucleophilc attack of CN^- to DMAD-0 and DMAD-90.

Finally, the site activation model discussed above was contrasted with the actual activation scheme displayed by the transition structures **TSc−I** and **TS1−I** for the concerted and stepwise mechanism, respectively. The results are included in entries v and vi in Table 5. It may be seen that in general a similar activation pattern as the one shown by the model using

CN^- is obtained. For **TSc−I**, the local electrophilic and nucleophilic responses at sites C5 and C6 are equivalent, as a result of the highly symmetric TS structure. Note that the low electrophilic deactivation shown at sites C5 and C6 (compare column 4 entries i and v) is consistent with the low charge-transfer pattern shown by these atomic centers quoted in Table 2. Site activation at the **TS1−I** structure on the other hand shows a strong nucleophilic activation at C6 and a lower electrophilic and nucleophilic activation at C5. Note that activation in nucleophilic softness at C6 (last column sixth entry in Table 5) is even greater than the one shown by the model including CN^- as nucleophile. The enhancement in local softness at this site is also consistent with the charge-transfer pattern of **TS1−I** displayed in Table 2, as local softness is a regional measure of the charge capacity of the complex.

Conclusion

The molecular mechanisms for the cycloaddition reactions of 1,3-butadiene, (*E*)- and (*Z*)-1,3-pentadiene, and 4-methyl-1,3-pentadiene with dimethyl acetylenedicarboxylate (DMAD) have been studied using DFT methods. For these cycloaddition reactions, two-competitive mechanisms have been characterized: the first one corresponds to a concerted process where the asynchronicity in the C−C bond-formation depends on the methyl substitution. The second one corresponds to a stepwise process where a C−C bond is first formed along the nucleophilic attack of 1,3-butadiene system to a conjugate position of the substituted acetylene.

Two opposite factors are responsible for the relative energies associated to these competitive channels. The first one is associated to the increase of the nucleophilic character of 1,3-BDs with the presence of the electron-releasing methyl groups that favors the polar stepwise processes. The second one is a destabilization of the corresponding TSs because hindrance imposed by the presence of a larger methyl group. Thus, whereas 1,3-butadiene prefers the concerted process, substitution of hydrogen atoms by electron-releasing methyl groups at the 1,3-BDs favors the stepwise mechanisms along with an increase of the charge-transfer process.

The arrangement of the two-carboxylate groups, planar or perpendicular, has a decisive role at the stabilization of the corresponding TSs along the two competitive reactive channels. Although the planar arrangement activates the π acetylenic system involved at the concerted bond-formation processes, the perpendicular arrangement of the two-carboxylate groups favors the charge transfer associated to the C−C bond-formation along the stepwise processes. Inclusion of solvent effects by means of a polarizable continuum model does not modify these gas-phase results.

The DFT global analysis performed on DMAD shows that both planar and perpendicular conformations act as electrophile in the dienophile/diene interaction with these butadiene derivatives. The charge transfer is therefore predicted to take place from the diene toward the DMAD, as confirmed by the values of electronic chemical potential and charge transfer analysis at the corresponding TSs. Further, from the global electrophilicity difference between perpendicular DMAD and 1,3-butadiene, it may be predicted that the electrophile/nucleophile interaction will show a less ionic interaction than the one expected for methyl substituted butadienes. For the isolated DMAD, the planar conformation is globally more electrophilic than the perpendicular one. However, the local activation site analysis suggests that the perpendicular conformation is more favorable for the interaction with the nucleophile, because of a larger charge transfer when the two carboxylate groups are conjugated with each one of the two orthogonal π systems of the ethylene framework.

Acknowledgment. This work received partial financial support from the Ministerio de Educación y Cultura of the Spanish Government by DGICYT (project PB98-1429) and Fondecyt, Grants Nos. 3990033 and 1000816. R.C. thanks the Generalitat Valenciana for financial support (INV00-02-40) and Universidad de Valencia for the facilities made available to him and for the warm hospitality.

References and Notes

(1) Carruthers, W. *Some Modern Methods of Organic Synthesis*, 2nd ed.; Cambridge University Press: Cambridge, 1978.
(2) Carruthers, W. *Cycloaddition Reactions in Organic Synthesis*; Pergamon: Oxford, 1990.
(3) Sauer, J. *Angew. Chem., Int. Ed. Engl.* **1966**, *5*, 211.
(4) Sauer, J. *Angew. Chem., Int. Ed. Engl.* **1967**, *6*, 16.
(5) Sauer, J.; Sustmann, R. *Angew. Chem., Int. Ed. Engl.* **1980**, *19*, 779.
(6) Dewar, M. J. S.; Olivella, S.; Stewart, J. J. P. *J. Am. Chem. Soc.* **1986**, *108*, 5771.
(7) Houk, K. N.; González, J.; Li, Y. *Acc. Chem. Res.* **1995**, *28*, 81.
(8) Sakai, S. *J. Phys. Chem. A* **2000**, *104*, 922.
(9) Diels, O.; Alder, K. *Justus Liebigs Ann. Chem.* **1928**, *460*, 98.
(10) Woodward, R. B.; Hoffmann, R. *Angew. Chem., Int. Ed. Engl.* **1969**, *8*, 781.
(11) Loncharich, R. J.; Brown, F. K.; Houk, K. N. *J. Org. Chem.* **1989**, *54*, 1129.
(12) Houk, K. N.; Loncharich, R. J.; Blake, J. F.; Jorgensen, W. L. *J. Am. Chem. Soc.* **1989**, *111*, 9172.
(13) Birney, D. M.; Houk, K. N. *J. Am. Chem. Soc.* **1990**, *112*, 4127.
(14) Jorgensen, W. L.; Dongchul, L.; Blake, J. F. *J. Am. Chem. Soc.* **1993**, *115*, 2936.
(15) Sustmann, R.; Sicking, W. *J. Am. Chem. Soc.* **1996**, *118*, 12562.
(16) Domingo, L. R.; Picher, M. T.; Andrés, J.; Safont; V. S. *J. Org. Chem.* **1997**, *62*, 1775.
(17) Sustmann, R.; Tappanchai, S.; Bandmann, H. *J. Am. Chem. Soc.* **1996**, *118*, 12555.
(18) Domingo, L. R.; Jones, R. A.; Picher, M. T. Sepúlveda-Arques, J. *Tetrahedron* **1995**, *51*, 8739.
(19) Domingo, L. R.; Picher, M. T.; Andrés, J.; Moliner, V.; Safont, V. S. *Tetrahedron* **1996**, *52*, 10693.
(20) Domingo, L. R.; Picher, M. T.; Zaragozá, R. J. *J. Org. Chem.* **1998**, *63*, 9183.
(21) Domingo, L. R.; Picher, M. T.; Aurell, M. J. *J. Phys. Chem. A* **1999**, *103*, 11425.
(22) Domingo, L. R.; Picher, M. T.; Andrés, J. *J. Org. Chem.* **2000**, *65*, 3473.
(23) Sauer, J.; Wiest, H.; Mielert, A. *Chem. Ber.* **1964**, *97*, 3183.
(24) Froese, R. D. J.; Coxon, J. M.; West, S. C.; Morokuma, K. *J. Org. Chem.* **1997**, *62*, 6991.
(25) Abad, A.; Aguló, C.; Castelblanque, L.; Cuñat, A. C.; Navarro, I.; Ramírez de Arellano, M. C. *J. Org. Chem.* **2000**, *65*, 4189.
(26) Parr, R. G.; Yang, W. *Density Functional Theory of Atoms and Molecules*; Oxford University Press: New York, 1989.
(27) Parr, R. G.; Pearson, R. G. *J. Am. Chem. Soc.* **1983**, *105*, 7512.
(28) Pearson, R. G. *Chemical Hardness; Applications from Molecules to Solids*; Wiley-VHC, Verlag GMBH: Weinheim, Germany, 1997.
(29) Parr, R. G.; von Szentpaly, L.; Liu, S. *J. Am. Chem. Soc.* **1999**, *121*, 1922.
(30) Yang, W.; Mortier, W. J. *J. Am. Chem. Soc.* **1986**, *108*, 5708.
(31) Gázquez, J. L.; Méndez, F. *J. Phys. Chem.* **1994**, *98*, 4591.
(32) Pérez, P.; Contreras, R. *Chem. Phys. Lett.* **1998**, *292*, 239.
(33) Contreras, R.; Domingo, L. R.; Andrés, J.; Pérez, P.; Tapia, O. *J. Phys. Chem.* **1999**, *103*, 1367.
(34) Frisch, M. J.; Trucks, G. W.; Schlegel, H. B.; Scuseria, G. E.; Robb, M. A.; Cheeseman, J. R.; Zakrzewski, V. G.; Montgomery, J. A., Jr.; Stratmann, R. E.; Burant, J. C.; Dapprich, S.; Millam, J. M.; Daniels, A. D.; Kudin, K. N.; Strain, M. C.; Farkas, O.; Tomasi, J.; Barone, V.; Cossi, M.; Cammi, R.; Mennucci, B.; Pomelli, C.; Adamo, C.; Clifford, S.; Ochterski, J.; Petersson, G. A.; Ayala, P. Y.; Cui, Q.; Morokuma, K.; Malick, D. K.; Rabuck, A. D.; Raghavachari, K.; Foresman, J. B.; Cioslowski, J.; Ortiz, J. V.; Stefanov, B. B.; Liu, G.; Liashenko, A.; Piskorz, P.; Komaromi, I.; Gomperts, R.; Martin, R. L.; Fox, D. J.; Keith, T.; Al-Laham, M. A.; Peng, C. Y.; Nanayakkara, A.; Gonzalez, C.; Challacombe, M.; Gill, P. M. W.; Johnson, B. G.; Chen, W.; Wong, M. W.; Andres, J. L.; Head-Gordon, M.; Replogle, E. S.; Pople, J. A. *Gaussian 98*, revision A.1; Gaussian, Inc.: Pittsburgh, PA, 1998.

(35) Sbai, A.; Branchadell, V.; Oliva, A. *J. Org. Chem.* **1996**, *61*, 621.
(36) Ziegler, T. *Chem. Rev.* **1991**, *91*, 651.
(37) Becke, A. D. *J. Chem. Phys.* **1993**, *98*, 5648.
(38) Lee, C.; Yang, W.; Parr, R. G. *Phys. Rev. B* **1988**, *37*, 785.
(39) Hehre, W. J.; Radom, L.; Schleyer, P. v. R.; Pople, J. A. *Ab Initio Molecular Orbital Theory*; Wiley: New York, 1986.
(40) Stanton, R. V.; Merz, K. M. *J. Chem. Phys.* **1994**, *100*, 434.
(41) Carpenter, J. E.; Sosa, C. P. *THEOCHEM* **1994**, *311*, 325.
(42) Goldstein, E.; Beno, B.; Houk, K. N. *J. Am. Chem. Soc.* **1996**, *118*, 6036.
(43) Sbai, A.; Branchadell, V.; Ortuño, R. M.; Oliva, A. *J. Org. Chem.* **1997**, *62*, 3049.
(44) Martínez-Merino, V.; Mayoral, J. A.; Salvatella, L. *J. Am. Chem. Soc.* **1998**, *120*, 2415.
(45) Jursic, B.; Zdravkovski, Z. *J. Chem. Soc., Perkin Trans. 2* **1995**, 1223.
(46) Domingo, L. R.; Arnó, M.; Andrés, J. *J. Am. Chem. Soc.* **1998**, *120*, 1617.
(47) Schlegel, H. B. *J. Comput. Chem.* **1982**, *3*, 214.
(48) Schlegel, H. B. Geometry Optimization on Potential Energy Surface. In *Modern Electronic Structure Theory*; Yarkony, D. R., Ed.; World Scientific Publishing: Singapore, 1994.
(49) Scott, A. P.; Radom, L. *J. Phys. Chem.* **1996**, *100*, 16502.
(50) McIver, J. W. J.; Komornicki, A. *J. Am. Chem. Soc.* **1972**, *94*, 2625.
(51) Fukui, K. *J. Phys. Chem.* **1970**, *74*, 4161.
(52) González, C.; Schlegel, H. B. *J. Phys. Chem.* **1990**, *94*, 5523.
(53) González, C.; Schlegel, H. B. *J. Chem. Phys.* **1991**, *95*, 5853.
(54) Reed, A. E.; Weinstock, R. B.; Weinhold, F. *J. Chem. Phys.* **1985**, *83*, 735.
(55) Reed, A. E.; Curtiss, L. A.; Weinhold, F. *Chem. Rev.* **1988**, *88*, 899.
(56) Kahn, S. D.; Hehre, W. J.; Pople, J. A. *J. Am. Chem. Soc.* **1987**, *109*, 1871.
(57) Domingo, L. R.; Arnó, M.; Andrés, J. *J. Org. Chem.* **1999**, *64*, 5867.
(58) Tomasi, J.; Persico, M. *Chem. Rev.* **1994**, *94*, 2027.
(59) Simkin, B. Y.; Sheikhet, I. *Quantum Chemical and Statistical Theory of Solutions-A Computational Approach*; Ellis Horwood: London, 1995.
(60) Cossi, M.; Barone, V.; Cammi, R.; Tomasi, J. *Chem. Phys. Lett.* **1996**, *255*, 327.
(61) Cances, M. T.; Mennunci, V.; Tomasi, J. *J. Chem. Phys.* **1997**, *107*, 3032.
(62) Barone, V.; Cossi, M.; Tomasi, J. *J. Comput. Chem.* **1998**, *19*, 404.
(63) Contreras, R.; Fuentealba, P.; Galván, M.; Pérez, P. *Chem. Phys. Lett.* **1999**, *304*, 405.
(64) Fuentealba, P.; Pérez, P.; Contreras, R. *J. Chem. Phys.* **2000**, *113*, 2544.
(65) The reaction between Cp and DMAD has been also studied in order to test the B3LYP/6-31G* energetic results. For this cycloaddition only one highly asynchronous TS similar to **TSnc-II** has been found (see Figure 2). The potential energy barrier, 15.2 kcal/mol, is in a good agreement with the experimental value, 13.8 kcal/mol.[23] The lowering of the barrier relative to the reaction with (*E*)-1,3-pentadiene **II** is mainly due to the s-cis fused conformation of Cp; the barrier for the cycloaddition between the s-cis conformation of **II** and DMAD along **TSnc-II** is 15.2 kcal/mol.

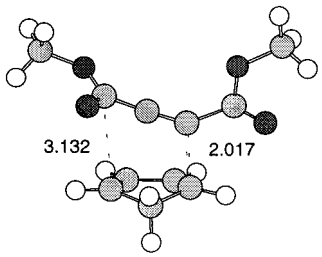

(66) Domingo, L. R.; Aurell, M. J.; Pérez, P.; Contreras, R. **2001**. Submitted for publication.
(67) Wiberg, K. B. *Tetrahedron* **1968**, *24*, 1083.
(68) For a discussion of the terminology used here, see cite 2 in ref 6.
(69) Domingo, L. R. *J. Org. Chem.* **2001**, *66*, 3211.